eISSN 2005-5447
International Journal of Stem Cells Vol. 17, No. 4, 2024 https://doi.org/10.15283/ijsc24089

ORIGINAL ARTICLE

Efficient Treatment of Psoriasis Using Conditioned Media from Mesenchymal Stem Cell Spheroids Cultured to Produce Transforming Growth Factor-β1-Enriched Small-Sized Extracellular Vesicles

Myeongjin Song[1,2], Kyung Min Lim[1,2], Kwonwoo Song[1,2], Geun-Ho Kang[1,2], Se Jong Kim[1,2], Youngseo Lee[1], Sujin Yu[1], Ki-Heon Jeong[3], Ssang-Goo Cho[1,2]

[1]*Department of Stem Cell and Regenerative Biotechnology, Molecular & Cellular Reprogramming Center and Institute of Advanced Regenerative Science, Konkuk University, Seoul, Korea*
[2]*R&D Team, StemExOne Co., Ltd., Seoul, Korea*
[3]*Department of Dermatology, College of Medicine, Kyung Hee University, Seoul, Korea*

Psoriasis is a common chronic inflammatory disease in which keratinocytes proliferate abnormally due to excessive immune action. Psoriasis can be associated with various comorbidities and has a significant impact on health-related quality of life. Although many systemic treatments, including biologic agents, have been developed, topical treatment remains the main option for psoriasis management. Consequently, there is an urgent need to develop topical treatments with minimal side effects and high efficacy. Mesenchymal stem cells (MSCs) exhibit excellent immune regulation, anti-inflammatory activities, and therapeutic effects, and MSC-derived extracellular vesicles (EVs) can serve as crucial mediators of functional transfer from MSCs. Therefore, this study aimed to develop a safe and easy-to-use emulsion cream for treating psoriasis using MSC conditioned media (CM) containing EVs. We developed an enhanced Wharton's jelly MSC (WJ-MSC) culture method through a three-dimensional (3D) culture containing exogenous transforming growth factor-β3. Using the 3D culture system, we obtained CM from WJ-MSCs, which yielded a higher EV production compared to that of conventional WJ-MSC culture methods, and investigated the effect of EV-enriched 3D-WJ-MSC-CM cream on psoriasis-related inflammation. Administration of the EV-enriched 3D-WJ-MSC-CM cream significantly reduced erythema, thickness, and scaling of skin lesions, alleviated imiquimod-induced psoriasiform lesions in mice, and ameliorated histopathological changes in mouse skin. The upregulated mRNA expression of inflammatory cytokines, including IL-17a, IL-22, IL-23, and IL-36, decreased in the lesions. In conclusion, we present here a new topical treatment for psoriasis using an MSC EV-enriched cream.

Keywords: Psoriasis, Extracellular vesicles, Mesenchymal stem cells, Emulsions, Immunomodulation

Received: July 29, 2024, Revised: August 13, 2024, Accepted: September 3, 2024, Published online: October 14, 2024

Correspondence to **Ssang-Goo Cho**
Department of Stem Cell and Regenerative Biotechnology, Molecular & Cellular Reprogramming Center and Institute of Advanced Regenerative Science, Konkuk University, 120 Neungdong-ro, Gwangjin-gu, Seoul 05029, Korea
E-mail: ssangoo@konkuk.ac.kr

Co-Correspondence to **Ki-Heon Jeong**
Department of Dermatology, College of Medicine, Kyung Hee University, 23 Kyungheedae-ro, Dongdaemun-gu, Seoul 02447, Korea
E-mail: khjeong246@khu.ac.kr

Introduction

Psoriasis is a common, chronic inflammatory disease characterized by abnormal keratinocyte proliferation due to excessive immune action and histological symptoms of hyperkeratosis, acanthosis, and parakeratosis (1). It presents with erythema and plaque and has comorbid diseases, such as arthritis and inflammatory bowel disease (2, 3). The physical, emotional, and social effects of psoriasis are reported to be comparable to or even more severe than those observed in patients with heart disease, cancer, arthritis, and diabetes (4). Patients with psoriasis are more likely to experience depression due to psychological and social problems, and 7.2% of them consider suicide (5). When patients with psoriasis are treated, symptoms of depression are often significantly reduced (6). Therefore, understanding and treating psoriasis are important.

Current clinical treatments for psoriasis are divided into local treatments, such as topical corticosteroids and vitamin D analogs, and systemic treatments, such as methotrexate (MTX), acitretin, and cyclosporine, depending on the disease severity. Local treatments are simple but cosmetically unappealing for daily use and lose efficacy over time; however, systemic treatments have a broader action but cause various side effects (7). For these reasons, biological agents are required for efficient treatment without side effects.

Mesenchymal stem cells (MSCs) are widely utilized in the treatment of various diseases due to their prominent features, including immunomodulatory, anti-inflammatory, and antitumor effects, cell suicide prevention, wound healing, and tissue recovery (8-11). Clinical and preclinical studies have demonstrated that MSC injections can significantly reduce the severity of psoriasis (12). However, as problems associated with cell therapy continue to emerge, new methods are required. Conditioned medium (CM) derived from MSCs is a new method that has therapeutic effects on psoriasis (13). In a recent study, effective factors within stem cells were packaged and delivered in signal transmission vesicles, known as extracellular vesicles (EVs), which typically range in size from 50～200 nm (14). Research using EV-enriched MSC CM has not been reported for psoriasis, and we thus considered creating MSC CM with a high concentration of EVs containing effective factors to enhance the therapeutic function of MSCs. To increase the yield of EVs derived from MSCs, methods including the addition of external substances, such as lipopolysaccharides (LPS) (15), thrombin (16), and eMTD (17), and changing the culture conditions to hypoxic (18) or three-dimensional (3D) environments (19). Our previous study showed that 3D culture methods and transforming growth factor-β3 (TGF-β3) addition enhanced EV production and the therapeutic efficacy of MSCs (19, 20). In the current study, our goal was to develop an easily applicable and side-effect-free treatment by producing MSC CM as an emulsion cream.

Materials and Methods

Cell culture

Isolation and characterization of Wharton's jelly MSCs (WJ-MSCs) were approved by the Institutional Review Board (7001355-202010-BR-407) of Konkuk University. (21). WJ-MSCs were cultured using CoreMAX MSC XF-AD (CM001-01; CORECELL), supplemented with 10% Serum Replacement (CM001-02; CORECELL) and 0.5% antibiotics (CM001-03; CORECELL), and maintained at 37℃ in a humidified atmosphere with 5% CO_2.

In our study, CM was produced from WJ-MSCs cultured via two-dimensional (2D) and 3D culture systems. For 2D-WJ-CM production, WJ-MSCs were seeded at 7×10^5 cells in a 175 mm dish (159910; Thermo Fisher Scientific) until they reached 80% confluency and then incubated at 37℃ with 5% CO_2 for four days in medium containing EV collection medium (M2001; RoosterBio). For 3D culture, AggreWell400 plates (ST34425; STEMCELL Technologies) were precoated with Rinsing solution (ST07010; STEMCELL Technologies). The plates precoated with Rinsing solution were centrifuged at 1500 *g* for 5 minutes to eliminate bubble. The rinsing solution from the plate was removed and each well was washed twice with 1 mL of phosphate-buffered saline (PBS) (10010023; Gibco). WJ-MSCs were suspended with EV collection medium and seeded at 1.5×10^6 cells/well in AggreWell400 plates that were precoated with Rinsing solution. The total EV collection medium volume per well was 3 mL. The cells cultured overnight at 37℃ with 5% CO_2 for the formation of MSC spheroids. The generated MSC spheroids were gently resuspended and washed with 1 mL of EV collection medium per well. The obtained cell suspension was centrifuged at 204 *g* for 1 minute to eliminate supernatant. The spheroids were then transferred to a 1 L Erlenmeyer flask (431147; Corning Inc.) containing 500 mL EV collection medium with added TGF-β3 (100-36E-10; PeproTech) at a concentration of 10 ng/mL. Next, we placed the MSC spheroid-containing flasks onto an orbital shaker with a sticky mat (69455, Celltron; INFORS HT) and subjected them to shaking at 100 rpm for four days in a humidified atmosphere at 37℃ with 5% CO_2.

Characterization of conditioned media

The size and concentration of EVs were measured using nanoparticle tracking analysis (NTA) with ZetaView (TWIN PMX-220; Particle Metrix) and the corresponding ZetaView 8.05.16 software. Before measurements, all the samples were diluted in 0.2 μm-filtered PBS in the range of 75~250 particles per frame for analysis. NTA was performed using the following settings: focus, auto; camera sensitivity, 80; frames per second, 30; shutter speed, 100; scattering intensity, detected automatically; and temperature, 22℃.

Protein quantification of CM was performed using a BCA protein assay kit (23225; Thermo Fisher Scientific), following the manufacturer's protocol.

Production of EVs

To isolate EVs from the culture supernatant, differential centrifugation was employed after 2D or 3D cell culture. The supernatant was centrifuged at 300 *g* for 10 minutes to eliminate cell debris. Subsequently, another centrifugation step at 2,000 *g* for 10 minutes was performed to remove the remaining debris. This was followed by a 30-minute centrifugation at 10,000 *g*. Finally, ultracentrifugation was carried out at 178,000 *g* for 2 hours at 4℃ to precipitate the EVs.

ELISA

For the TGF-β1 ELISA assay, we loaded 1×10^9 particles of EVs diluted in PBS into one well that had been coated with human TGF-β1 DuoSet (DY-240-05; R&D Systems) and Capture AB solution using the Ancillary Reagent Kit 1 (DY007; R&D system), following the manufacturer's protocol. First, non-coated wells were loaded with 100 μL Capture AB solution (2 μg/mL) and incubated overnight at room temperature (RT). Following incubation, the coated wells were blocked, whereafter 100 μL standards or samples containing EVs were added for a 2-hour incubation at RT. Subsequently, 100 μL Detection AB (50 ng/mL) was introduced, followed by another 2-hour incubation at RT. Then, streptavidin-HRP conjugate was added. After a 20-minute incubation with substrate solution at RT, the reaction was terminated with the addition of 50 μL stop solution. Finally, the absorbance was measured at a wavelength of 450 nm using a microplate reader.

To quantify the levels of mTNF-α (BGK06804; Peprotech), mIL-6 (BGK08505; Peprotech), and mIL-1β (BGK10749; Peprotech), ELISA assays were performed according to the manufacturer's protocol. Briefly, 100 μL of cell culture supernatant was added to antibody-coated wells and incubated at 37℃ for 90 minutes. Subsequently, the wells were incubated with biotinylated secondary antibody followed by avidin-biotin-peroxidase complex. We then added a color-developing reagent incubated for 10 to 30 minutes and finally added the stop solution to terminate the reaction. Finally, the absorbance was measured at a wavelength of 450 nm using a microplate reader.

Cell characterization

For the measurement of changes in immunophenotypic properties of the WJ-MSCs after 3D culture and TGF-β3 treatment, we measured the expression levels of surface markers using FACS analysis. The cells were trypsinized using 0.25% trypsin-EDTA (Gibco) and centrifuged at 459 *g* for 5 minutes. After removing the supernatant, the cell pellet was suspended in D-PBS containing 2% FBS, in which the primary antibodies were diluted by 1 : 200. The primary antibodies used were anti-CD90 (AF2067; R&D Systems), anti-CD105 (MA5-11854; Invitrogen), and anti-CD45 (130-110-771; Miltenyi Biotec). Cells were allowed to bind to the primary antibodies for 1 hour and 30 minutes at 4℃, which was followed by a washing step with PBS via centrifugation at 165 *g* for 5 minutes. The cells were then incubated with secondary antibodies, including goat anti-mouse IgG (A28175; Invitrogen) and donkey anti-sheep IgG (ab7009; Abcam) for 1 hour and 30 minutes at 4℃, followed by washing with PBS. Flow cytometry (CytoFLEX; Beckman Coulter) was used to measure fluorescence intensities of the labeled antibodies.

Table 1. The ingredient of emulsion components

%w/w	Ingredient							
	DW	Olive oil	MTX	2D-WJ-CM	3D-WJ-CM	Polysorbate-60	Carbopol-980	Total
PBS	46.200	50	-	-	-	3	0.8	100
MTX	46.175	50	0.025	-	-	3	0.8	100
2D	14.475	50	-	31.725	-	3	0.8	100
3D	7.015	50	-	-	39.185	3	0.8	100

DW: distilled water, MTX: methotrexate, 2D: two-dimensional, WJ: Wharton's jelly, 3D: three-dimensional, CM: conditioned media, PBS: phosphate-buffered saline.

Emulsion cream production

The ingredient of emulsion components for each group is shown in Table 1. Rheodol TW-S120V (polysorbate-60; Kao Chemicals) and extra virgin olive oil (Kerfoot) were added to a 1 L beaker and mixed for 10 minutes with a stirrer (HS-50A; DAIHAN Scientific) at 1,500 rpm. After the addition of distilled water (DW), MSC CM or MTX was introduced and mixed for 10 minutes under the same conditions at 1,500 rpm. Finally, Carbopol 980 (Carbomer; WhatSoap) was added and mixed for 15 minutes at 2,000 rpm.

Mice and *in vivo* experiments

Eight-week-old BALB/c mice (female, 20±2 g) were purchased from JA BIO. All experimental procedures were approved by the Institutional Animal Care and Use Committee (IACUC) of Konkuk University (IACUC: KU23104). All animals were housed for one week before the experiment for proper acclimatization in a well-ventilated room with adjusted temperature and humidity and a 12 hours light/12 hours dark cycle. Food and water were provided ad libitum.

Mice received a daily topical dose of 50 mg commercially available imiquimod (IMQ) cream (5%) (Aldara; 3M Pharmaceuticals) on their shaved backs for six consecutive days. To measure the therapeutic potency of the emulsion cream, we divided the mice into five groups as follows: (1) normal (IMQ untreated control), (2) vehicle (PBS) cream-treated, (3) MTX cream-treated, (4) 2D-WJ-CM cream-treated, and (5) 3D-WJ-CM cream-treated groups (n=8 mice/group). We applied 130 mg emulsion cream to shaved backs of the mice for three consecutive days. The doses added for each were as follows in 130 mg of the emulsion cream: 2D- and 3D-MSC secretome were treated with 50 μg based on protein volume, and MTX treated with 5 mg/kg. Subsequently, the animals were euthanized for RNA expression and histological analyses. Erythema, scaling, and thickness of the back skin were scored independently every day on a scale of 0～4 (22). To score the severity of back skin inflammation, we used the clinical psoriasis area and severity index. However, for the mouse model, the skin area of psoriasis was not considered. Erythema, dead skin cells, and skin thickness were scored from 0～4, which represented the following: 0, none; 1, slight; 2, normal; 3, severe; 4, very severe.

Histological analysis

Skin tissues were collected and fixed using 4% paraformaldehyde (PFA) in PBS, followed by rinsing with PBS to remove PFA traces. The tissue was then transferred into a mold with an optimal cutting temperature (OCT) compound (Tissue-Tek), with careful orientation of the tissue. Then, it was placed over dry ice for several minutes for equilibration and subsequently stored at −80℃ until cryosectioning. For cryosectioning, the samples were mounted on a specimen chuck with OCT compound and then loaded onto the cryostat object holder, with the holder blade adjusted relative to the sample. The tissue blocks were then cut into 3-μm sections and stained with H&E. H&E data were analyzed using SlideViewer 2.7.0.191696 software.

RNA isolation, cDNA synthesis, and reverse transcription-polymerase chain reaction analysis

Skin tissues were homogenized, and total RNA isolated from the tissues using LaboZol reagent (CMRZ001; LaboPass), according to the manufacturer's instructions. The purified RNA was quantified using a NanoDrop spectrophotometer (ND-ONE; NanoDrop Technologies, Inc.). The cDNA was synthesized from 2 μg total RNA using an M-MuLV reverse transcription kit (CMRT010; Labopass) and oligo dT primers. Polymerase chain reaction (PCR) was performed using the HiPi Real-Time PCR 2× Master Mix (SYBR green, ROX) (EBT-1802; ELPISBIO). The primers were designed using Primer3 (ver. 4.1.0) as follows: TLR7, F: 5'-GTGATGCTG TGTGGTTTG TCTGG-3', R: 5'-CCTTTGTGTGCTCCTGGACCTA-3'; IL-17a, F: 5'- CAGACTACCTCAACCGTTCC AC-3', R: 5'-TCCAGCTTTCCCTCCGCATTGA-3'; IL-23a, F: 5'-CA TGCTAGCCTGGAACGCACAT-3', R: 5'-ACTGGCTG TTGTCCTTGAGTCC-3'; IL-22, F: 5'- GCTTGAGGTG TCCAACTTCCAG-3', R: 5'-TCCAGCTTTCCCTCCGC ATTGA-3'; IL-36, F: 5'- TTGACTTGGACC AGCAGGTGTG-3', R: 5'- GGGTACTTGCATGGGAG GATAG-3'.

Measurement of nitric oxide production

RAW 264.7 cells were seeded at a density of 1.5×10^5 cells per well in 24-well plates (30024; SPL) and cultured overnight in incubator at 37℃ with 5% CO_2. Cells were then stimulated with LPS (derived from Escherichia coli O111:B4, L4391; Sigma-Aldrich), MTX, and EVs in DMEM high glucose medium (D6429; Sigma-Aldrich) supplemented with 10% EV-depleted FBS. LPS was added at a concentration of 10 ng/mL, and MTX was added at a concentration of 10 μM. After 24 hours of stimulation, culture supernatants were collected and centrifuged at 200 *g* for 3 minutes to remove cellular debris. Nitric oxide (NO) levels were determined using the Griess reagent system. Briefly, equal volumes of supernatant and Griess reagent (a 1 : 1 mixture of 0.1% N-(1-naphthyl) ethylenediamine dihydrochloride [33461; Sigma-Aldrich] and 1% sulfanilamide [S9251; Sigma-Aldrich] in 5% phosphoric acid [345245;

Sigma-Aldrich]) were incubated for 15 minutes at RT. Absorbance was measured at 540 nm using a microplate reader.

Statistical analysis

Statistical analyses were performed using GraphPad Prism (GraphPad Software). Data are displayed as the mean±SEM. Unpaired two-tailed Student's t-test (two groups) and one-way or two-way ANOVA with Tukey's post-hoc test (more than two groups) were performed to compare values and evaluate statistical significance. Statistical significance was set at $p<0.05$.

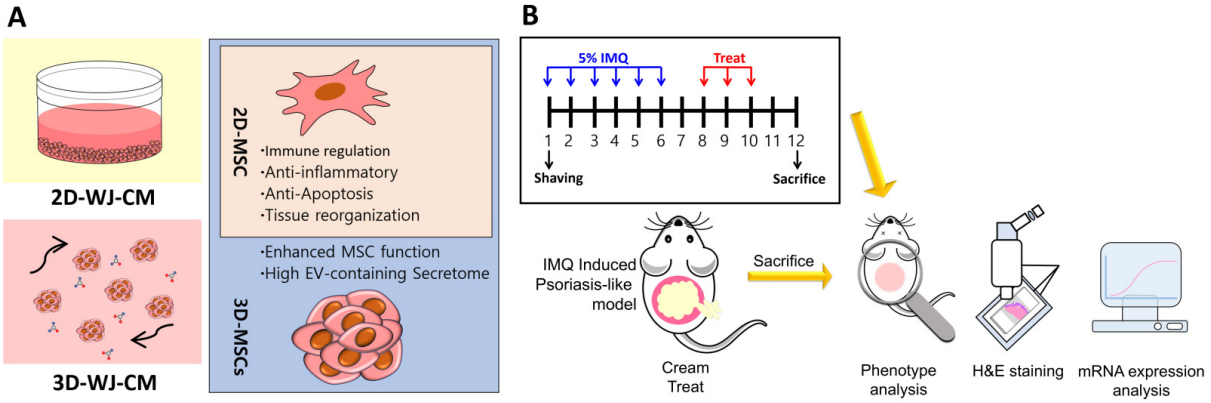

Fig. 1. Schematic diagram of the topical treatment. (A) Differences in the 2D and 3D culture methods, as well as the advantages of MSCs and 3D MSCs. The arrow represents the shaking motion applied to the culture medium within the culture flask. (B) Schedule of the cream processing and experimental procedures. IMQ was topically applied from days 0~6, and MSC conditioned media cream applied from days 8~10. The experiment was terminated on day 12. 2D: two-dimensional, WJ: Wharton's jelly, CM: conditioned media, 3D: three-dimensional, MSCs: mesenchymal stem cells, IMQ: imiquimod.

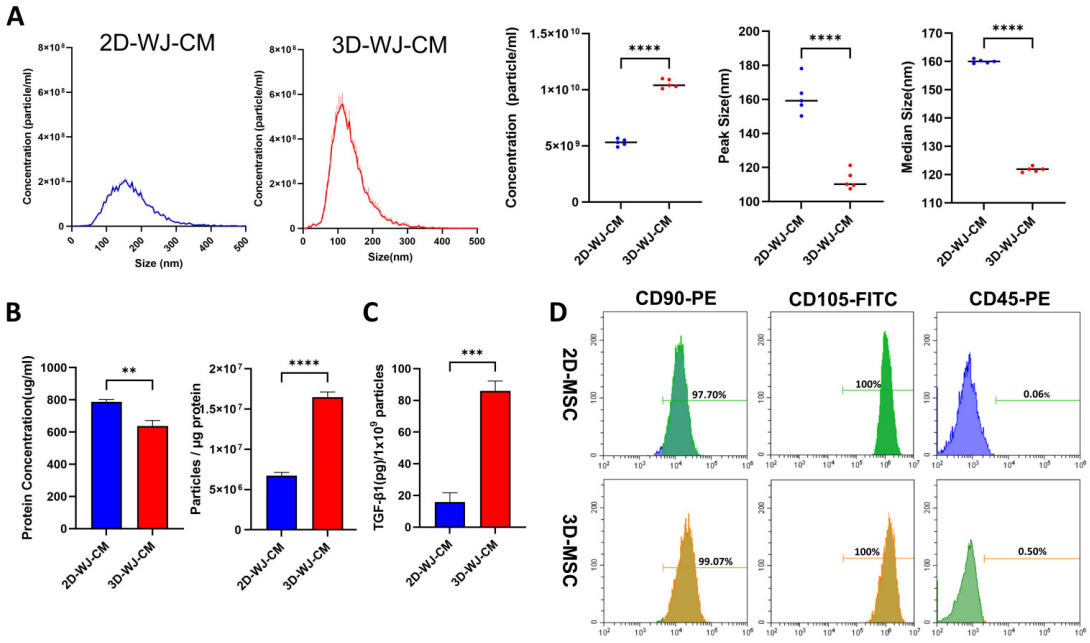

Fig. 2. Characterization of WJ-MSCs and their CM. (A) Comparative analysis of nanoparticles in 2D-WJ-CM and 3D-WJ-CM. The distribution of nanoparticles by size, total concentration per milliliter, peak size (nm), and median size (nm) were measured using ZetaView (TWIN PMX-220; Particle Metrix). (B) Comparison of protein volume and their EV purity (particle number/protein concentration) in 2D-WJ-CM and 3D-WJ-CM. (C) Total expression of TGF-β1 per 1×10^9 particles in EVs. TGF-β1 levels were significantly higher in 3D-WJ-CM compared to those in 2D-WJ-CM. (D) Flow cytometry analysis of MSC-positive surface marker CD90/105 and negative surface marker CD45 in 2D-MSCs and 3D-MSCs. 2D: two-dimensional, WJ: Wharton's jelly, CM: conditioned media, 3D: three-dimensional, MSC: mesenchymal stem cell, EV: extracellular vesicle, TGF-β1: transforming growth factor-β1. Results with a p-value<0.05 were considered statistically significant. **p<0.01, ***p<0.001, ****p<0.0001.

Results

Characterization of WJ-MSCs and their conditioned media

We obtained WJ-MSC CM produced in 3D spheroids stimulated with TGF-β. Culturing the WJ-MSCs in 3D form enhanced several of their functions and increased the production of nanoparticles (Fig. 1A). To induce psoriasis, we applied IMQ cream for six days and then treated the cream for three days. The WJ-MSC CM were prepared in the form of an emulsion cream and used to treat the backs of hair-removed mice. After the animal experiments were completed, phenotypic, histological, and mRNA analyses were performed (Fig. 1B).

We measured the nanoparticle and protein concentrations in both 2D-WJ-CM and 3D-WJ-CM. 3D-WJ-CM had about 2.7 times more nanoparticles than 2D-WJ-CM did, showing a smaller mode and median size (Fig. 2A). The protein concentration in 2D-WJ-CM was about 1.2 times higher than that in 3D-WJ-CM (Fig. 2B). 3D-WJ-CM contained approximately 3.2 times more nanoparticles than 2D-WJ-CM did when treated with the same protein concentration. In conclusion, the purity of samples containing EVs was highest in 3D-WJ-CM (Fig. 2B). Moreover, EVs derived from 3D-WJ-CM treated with TGF-β3 exhibited higher TGF-β1 expression (Fig. 2C).

For assessing changes in immunophenotypic properties of the WJ-MSCs produced in 3D spheroids stimulated physically with TGF-β3, we measured the expression levels of surface markers using FACS analysis. Finally, we analyzed the expression levels of the positive MSC markers using FACS analysis, which revealed that those of CD90-PE and CD105-FITC were similar in the 2D-MSC and 3D-MSC groups (Fig. 2D).

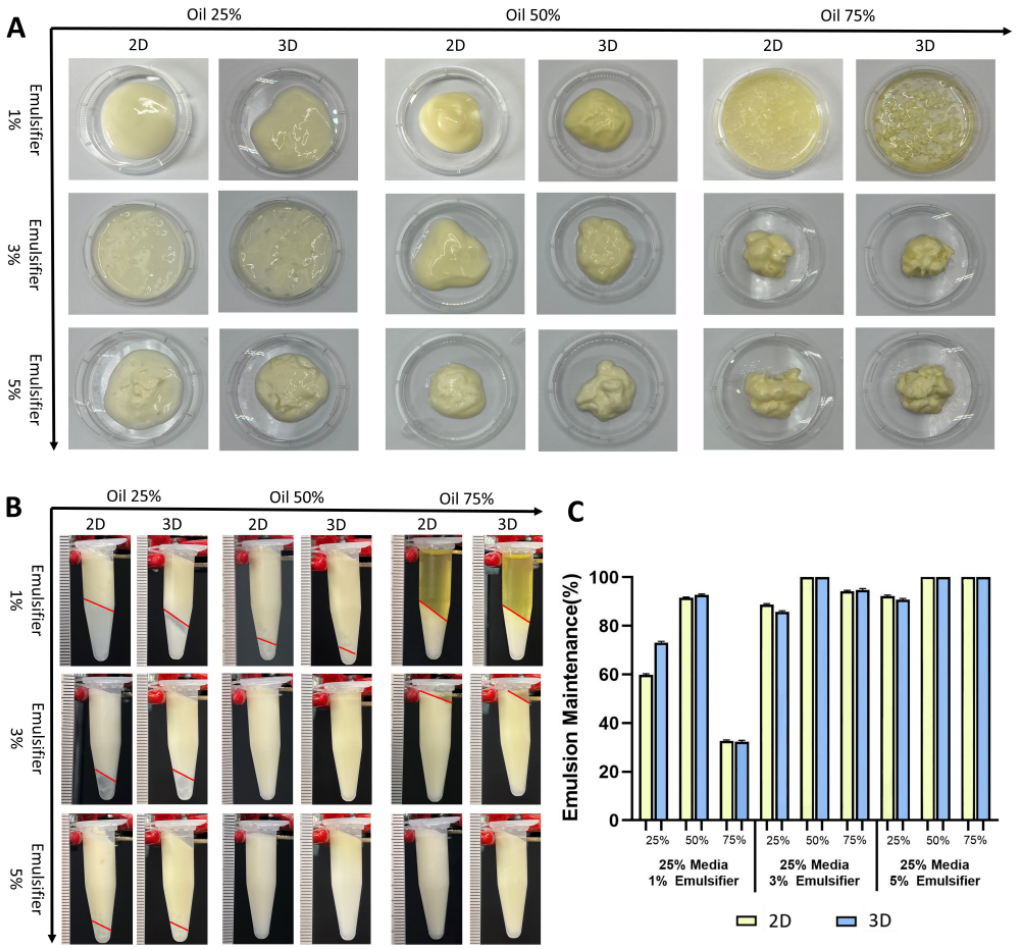

Fig. 3. Emulsion cream selection. (A) Formulation shape according to oil and emulsifier ratios in 2D-WJ-CM and 3D-WJ-CM. (B) The degree of phase separation according to oil and emulsifier ratios in 2D-WJ-CM and 3D-WJ-CM. The left-angled red line indicates the phase-separated position. (C) Proportion of maintaining the emulsion form. 2D: two-dimensional, WJ: Wharton's jelly, CM: conditioned media, 3D: three-dimensional.

Optimal 3D-MSC CM emulsion cream formulation

To conduct the most convenient clinical trials for skin diseases, an emulsion cream formulation needs to be developed. Among the various CM conditions tested, we were able to determine the optimal formulation. Initially, we explored a formulation that maintained its shape to remain on back skin for a long period after application. When 25% oil was added, 5% emulsifier had to be used. When 50% oil was added, the cream formulation was maintained, regardless of the amount of emulsifier used. When 75% oil was added, at least 3% emulsifier had to be used to maintain the cream formulation (Fig. 3A). Next, we explored the degree of phase separation after emulsion cream production. When 25% oil was added, DW separation occurred in all emulsion creams. When 50% oil was added, DW separation occurred only when the emulsifier concentration was 1%. When 75% oil was added, oil separation occurred except when the emulsifier concentration was 5% (Fig. 3B, 3C). Among the three conditions that maintained the cream formulation and prevented phase separation (50% oil, 3% emulsifier; 50% oil, 5% emulsifier; and 75% oil, 5% emulsifier), the emulsifier, which is a detergent ingredient, could decompose lipid membranes (23). As the representative components of EVs are lipids, we selected the condition with 50% oil and 3% emulsifier because it contained the least amount of emulsifier. measure fluorescence intensities of the labeled antibodies.

3D CM emulsion cream recovered IMQ-induced psoriasis in mice

A phenotypic analysis was conducted to assess the therapeutic efficacy of 3D-WJ-CM. The skin color of the 3D-WJ-CM group closely resembled that of normal skin and appeared devoid of the stratum corneum. By contrast, the 2D-WJ-CM group exhibited red skin and lacked dead skin cells (Fig. 4A). Thickness, erythema, and scaling were scored to visualize therapeutic effects of the emulsion cream. Cumulative score analysis revealed that the 3D-WJ-CM group had the lowest score, indicating a more effective treatment of psoriasis compared to that of the other groups (Fig. 4B). In the vehicle group, hyperkeratosis, characterized by excessive keratinocyte proliferation in the stratum corneum, and parakeratosis, represented by retained nuclei in the stratum corneum, were clearly observed. Additionally, symptoms of acanthosis, marked by epidermal thickening, were evident. In contrast, in the group treated with 3D-WJ-CM, the symptoms improved significantly. In addition, the symptoms improved not only after 3D-WJ-CM treatment, but also when the natural 2D-WJ-CM cream was used (Fig. 5A). Treatment affected not only the mouse phenotype, but also the cytokine mRNA levels. IMQ is a ligand of TLR7 and TLR8 (24), and psoriasis-induced mice showed high TLR7 levels, whereas the mRNA levels of TLR were lowered when treated with the 3D-WJ-CM cream. The mRNA levels of IL-17α, IL-23α, IL-22, and IL-36, which are involved in downstream sig-

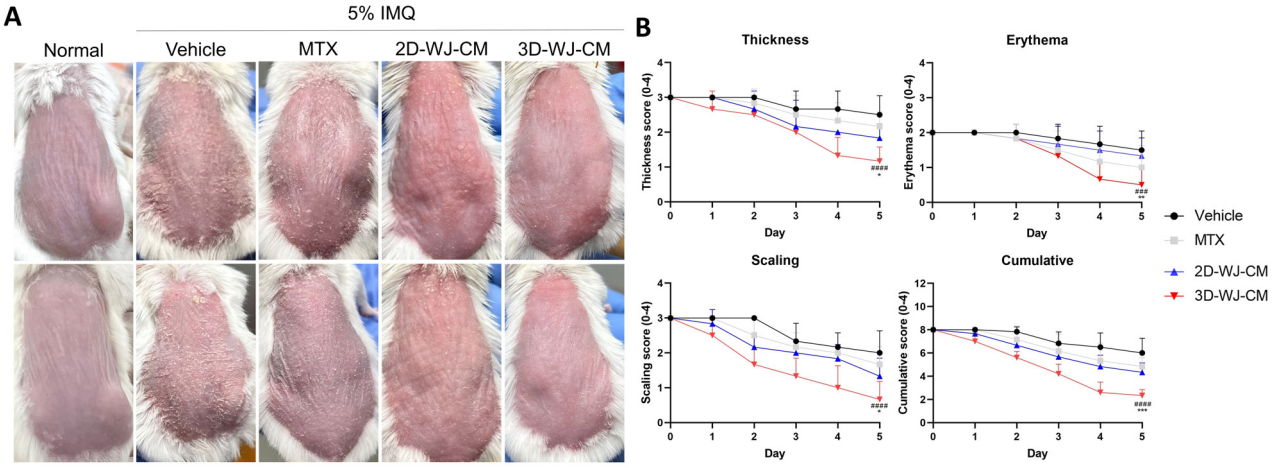

Fig. 4. Phenotype of 3D-WJ-CM cream-treated psoriasis-like mice. Mice were randomly divided into five groups: normal, IMQ+vehicle, IMQ+MTX, IMQ+2D-WJ-CM, and IMQ+3D-WJ-CM groups. (A) Two representative photographs of mice phenotypes before sacrifice. (B) In the back skin of BALB/c mice, the thickness, erythema, and scaling were scored from 0~4 points from the start of treatment to the date of sacrifice. In addition, the cumulative score combining thickness, erythema, and scaling was presented. Symbols represent the mean standard deviation of six mice. IMQ: imiquimod, MTX: methotrexate, 2D: two-dimensional, WJ: Wharton's jelly, CM: conditioned media, 3D: three-dimensional. Two-way ANOVA showed significant differences between groups, $^{###}p<0.001$, $^{####}p<0.0001$ compared to Vehicle and 3D-WJ-CM. $^{*}p<0.05$, $^{**}p<0.01$, $^{***}p<0.001$ compared to 2D-WJ-CM and 3D-WJ-CM.

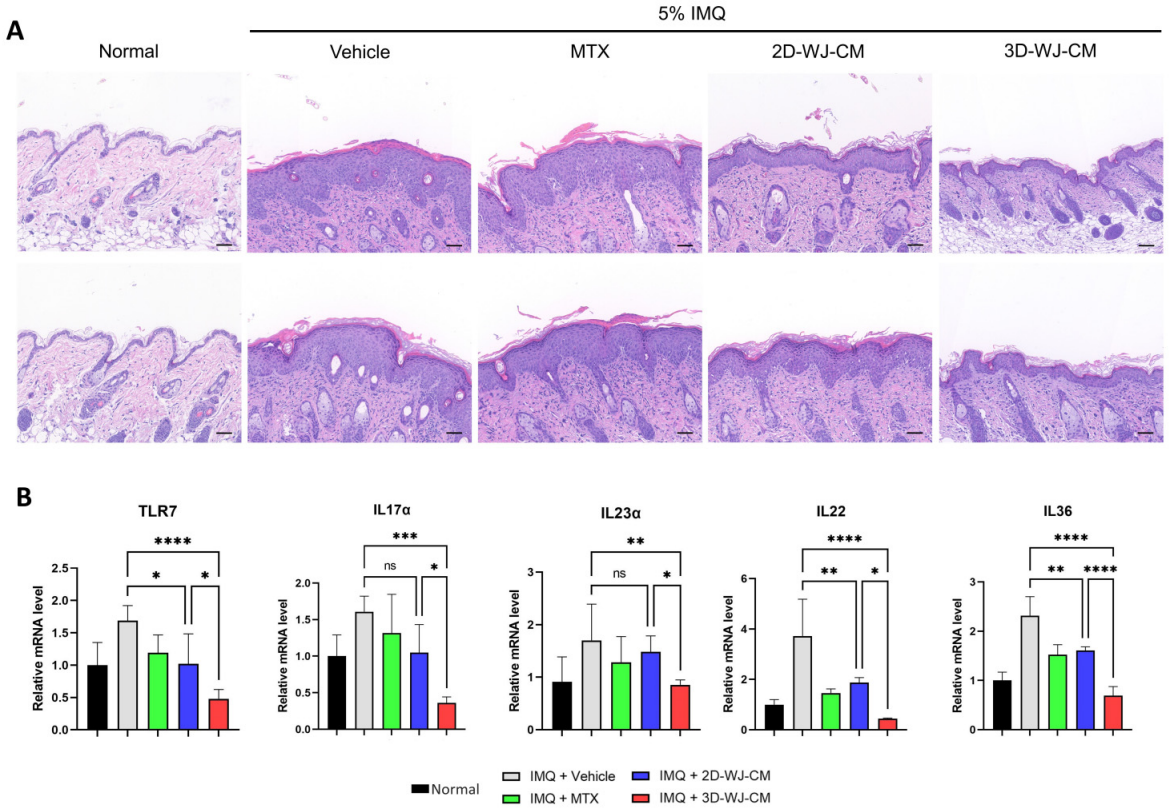

Fig. 5. 3D-WJ-CM cream recovery in psoriasis-like mice. (A) H&E staining of mice skin by group. Scale bar=50 μm. (B) Levels of inflammatory cytokines (TLR7, IL-17α, IL-23α, IL-22, and IL-36) in the back skin of psoriasis-like mice treated with 3D-WJ-CM. IMQ: imiquimod, MTX: methotrexate, 2D: two-dimensional, WJ: Wharton's jelly, CM: conditioned media, 3D: three-dimensional. Results with a p-value<0.05 were considered statistically significant. *p<0.05, **p<0.01, ***p<0.001, ****p<0.0001, and ns=not significant compared to the IMQ+vehicle group.

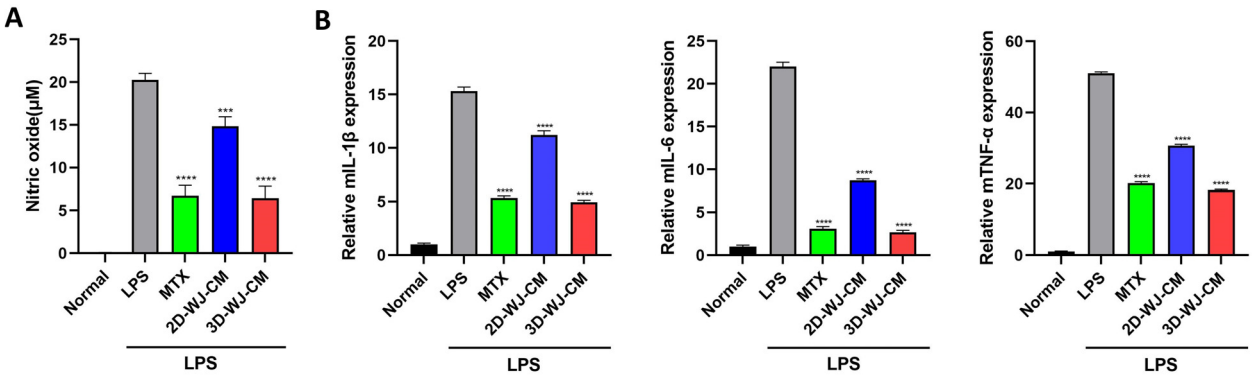

Fig. 6. 3D-WJ-CM attenuates inflammation *in vitro*. (A) The concentration of nitric oxide in the supernatant of LPS-stimulated RAW 264.7 cells. (B) Protein expression levels of inflammatory cytokines (IL-1β, IL-6, and TNF-α). Protein expression was detected in the cell supernatant by ELISA. LPS: lipopolysaccharide, MTX: methotrexate, 2D: two-dimensional, WJ: Wharton's jelly, CM: conditioned media, 3D: three-dimensional. ***p<0.001, ****p<0.0001 compared to the LPS group.

nals of TLR7 (25), were all downregulated (Fig. 5B). Thus, the 3D-WJ-CM cream penetrated the skin and effectively modulated the expression of sequential cytokines involved in psoriasis.

3D CM recovered inflammation to RAW 264.7 cell induced with LPS

To further investigate the anti-inflammatory effects of 3D-WJ-CM *in vitro*, we performed an inflammation assay using mouse macrophages. MTX effectively suppressed

NO production induced by LPS, and our 3D-WJ-CM showed a similar effect (Fig. 6A). When we examined inflammatory cytokines such as IL-1β, IL-6, and TNF-α, 3D-WJ-CM exhibited similar or even better inhibitory effects compared to MTX. In addition, 2D-WJ-CM also showed some degree of anti-inflammatory effects (Fig. 6B). These results indicate that our 3D-WJ-CM not only treats inflammatory skin diseases such as psoriasis when applied topically in cream form but also exhibits anti-inflammatory effects *in vitro*.

Discussion

MSCs have immunomodulatory and anti-inflammatory properties and can also prevent apoptosis, wound healing, and tissue repair (8-11). Research on the use of MSCs in various autoimmune diseases is currently underway (26), with ongoing preclinical and clinical trials investigating their potential in treating psoriasis (12). Specifically, MSCs can reduce disease severity, hyperkeratosis, immune cell infiltration, and proinflammatory cytokine production in psoriasis (27, 28).

However, a notable limitation to injecting MSCs *in vivo* is that the engrafted MSCs gradually disappear (29). In other words, if CM is used, various functional factors secreted by cells can be delivered to the cells without any problems related to cell injection. In our previous study, we added TGF-β3 to regulate mechanical force-related mechanisms (19). We have successfully produced TGF-β1-enriched EVs in 3D-MSC CM through a 3D culture with the addition of TGF-β3. Our EVs in 3D-MSC CM exhibited smaller peak and median sizes than those in conventional 2D CM. Studies have shown that smaller EVs are more readily taken up by cells (30). In addition, our EVs contained a high concentration of TGF-β1; some studies have shown that upregulation of TGF-β1 is helpful for psoriasis treatment (31-33). In conclusion, our 3D-MSC CM, comprising large amounts of small-sized EVs containing TGF-β1, could be highly effective in treating psoriasis.

Through a series of experiments conducted under various conditions, CM was successfully transformed into an optimized emulsion cream. If our cream were to be applied clinically, it could be more effective than general topical treatments are and may have fewer side effects than systemic treatments do because of the various functions exhibited by MSCs. When topically administering MSC CM as an emulsion, the degree of skin penetration must be considered. The molecular size should be smaller than 500 Da to effectively penetrate the skin barrier (34). As the molecular weight of MSC-driven EVs is greater than 100 kDa, they cannot penetrate the normal skin barrier (35). However, as the skin barrier in psoriasis-like mice does not maintain normal homeostasis, EVs and various biomolecules derived from MSCs are expected to pass through the skin.

Our emulsion cream effectively downregulated the expression of several upregulated mRNAs in psoriasis. When psoriasis is induced in mice, TLR7, an IMQ receptor, is activated (24). Myeloid dendritic cells (mDCs) then undergo maturation (25). These mature mDCs promote the production of IL-23, which in turn stimulates the activity of T17 helper cells and the secretion of IL-17 and IL-22 (25). In addition to inflammatory cytokines, psoriasis-induced keratinocytes secrete IL-36 to promote epidermal hyperplasia (25). In other words, our emulsion cream not only restored the phenotype and histology, but also restored the previously mentioned mRNA to normal levels. Moreover, a similar trend was observed *in vitro*. When macrophages were treated with LPS, they released NO, an indicator of inflammation (36), and 3D-WJ-CM exhibited anti-inflammatory effects similar to MTX. Furthermore, 3D-WJ-CM decreased the expression levels of inflammatory cytokines such as IL-1β, IL-6, and TNF-α released from LPS-treated RAW 264.7 cells. Given that chronic inflammatory skin diseases like psoriasis are characterized by the release of IL-1β, IL-6, and TNF-α (25, 37), 3D-WJ-CM is expected to contribute significantly to the treatment of psoriasis.

Conclusions

It was demonstrated that even when 3D-WJ-CM was administered in the form of an emulsion cream for topical treatment, it was more effective in treating psoriasis than 2D-WJ-CM was. Ultimately, we present here a new topical treatment for psoriasis through a WJ-MSC CM cream enriched with TGF-β1-containing small EVs. Our experiments have significant implications for psoriasis treatment and potentially for other skin conditions. As it showed better effects than steroid drugs did when prepared as creams, the WJ-MSC CM cream could serve as a good solution to both the shortcomings of general cream applications and the side effects of systemic treatments experienced by many patients. Finally, stem cell-derived CM contain a variety of factors, and further research should be conducted to identify the key factors that mediate its underlying mechanisms of action.

ORCID

Myeongjin Song, https://orcid.org/0009-0008-2450-2394

Kyung Min Lim, https://orcid.org/0000-0001-5456-255X
Kwonwoo Song, https://orcid.org/0000-0001-9150-4754
Geun-Ho Kang, https://orcid.org/0000-0002-7434-5672
Se Jong Kim, https://orcid.org/0009-0006-6607-2690
Youngseo Lee, https://orcid.org/0009-0003-3022-8807
Sujin Yu, https://orcid.org/0009-0001-0256-1261
Ki-Heon Jeong, https://orcid.org/0000-0001-6908-0932
Ssang-Goo Cho, https://orcid.org/0000-0002-0968-7932

Funding

This study was supported by the Konkuk University Researcher Fund in 2023 and by the Korean Fund for Regenerative Medicine grant funded by the Korean government (the Ministry of Science and ICT and the Ministry of Health & Welfare) (grant numbers: 22B0502L1- 01 and 24A0203L1 to SGC).

Potential Conflict of Interest

Ssang-Goo Cho is the CEO and CTO of StemExOne Co., Ltd. MS, KML, KS, GHK, and SJK are employed by StemExOne Co., Ltd. The other authors have no conflicts of interest to declare.

Authors' Contribution

Conceptualization: MS, KML, KHJ, SGC. Methodology: MS, KML, KS, KHJ, SGC. Supervision: SGC, KHJ. Project administration: SGC. Funding acquisition: SGC. Validation: GHK, SJK, YL, SY. Formal analysis: MS, KML, KS, GHK, SJK, YL, SGC. Writing – original draft: MS. Writing – review and editing: KML, KS, GHK, SJK, KHJ, SGC.

References

1. Wagner EF, Schonthaler HB, Guinea-Viniegra J, Tschachler E. Psoriasis: what we have learned from mouse models. Nat Rev Rheumatol 2010;6:704-714
2. Gulliver W. Long-term prognosis in patients with psoriasis. Br J Dermatol 2008;159 Suppl 2:2-9
3. Moll JM, Wright V. Psoriatic arthritis. Semin Arthritis Rheum 1973;3:55-78
4. Rapp SR, Feldman SR, Exum ML, Fleischer AB Jr, Reboussin DM. Psoriasis causes as much disability as other major medical diseases. J Am Acad Dermatol 1999;41(3 Pt 1):401-407
5. Gupta MA, Gupta AK. Depression and suicidal ideation in dermatology patients with acne, alopecia areata, atopic dermatitis and psoriasis. Br J Dermatol 1998;139:846-850
6. Tyring S, Gottlieb A, Papp K, et al. Etanercept and clinical outcomes, fatigue, and depression in psoriasis: double-blind placebo-controlled randomised phase III trial. Lancet 2006;367:29-35
7. Lebwohl M, Ting PT, Koo JY. Psoriasis treatment: traditional therapy. Ann Rheum Dis 2005;64 Suppl 2(Suppl 2): ii83-ii86
8. Toma C, Pittenger MF, Cahill KS, Byrne BJ, Kessler PD. Human mesenchymal stem cells differentiate to a cardiomyocyte phenotype in the adult murine heart. Circulation 2002;105:93-98
9. Baraniak PR, McDevitt TC. Stem cell paracrine actions and tissue regeneration. Regen Med 2010;5:121-143
10. Keating A. Mesenchymal stromal cells: new directions. Cell Stem Cell 2012;10:709-716
11. Li B, Zhang H, Zeng M, et al. Bone marrow mesenchymal stem cells protect alveolar macrophages from lipopolysaccharide-induced apoptosis partially by inhibiting the Wnt/β-catenin pathway. Cell Biol Int 2015;39:192-200
12. Paganelli A, Tarentini E, Benassi L, Kaleci S, Magnoni C. Mesenchymal stem cells for the treatment of psoriasis: a comprehensive review. Clin Exp Dermatol 2020;45:824-830
13. Yang M, Wang L, Chen Z, et al. Topical administration of the secretome derived from human amniotic epithelial cells ameliorates psoriasis-like skin lesions in mice. Stem Cell Res Ther 2022;13:393
14. Yáñez-Mó M, Siljander PR, Andreu Z, et al. Biological properties of extracellular vesicles and their physiological functions. J Extracell Vesicles 2015;4:27066
15. Ti D, Hao H, Tong C, et al. LPS-preconditioned mesenchymal stromal cells modify macrophage polarization for resolution of chronic inflammation via exosome-shuttled let-7b. J Transl Med 2015;13:308
16. Sung DK, Chang YS, Sung SI, Ahn SY, Park WS. Thrombin preconditioning of extracellular vesicles derived from mesenchymal stem cells accelerates cutaneous wound healing by boosting their biogenesis and enriching cargo content. J Clin Med 2019;8:533
17. Lim KM, Han JH, Lee Y, et al. Rapid production method with increased yield of high-purity extracellular vesicles obtained using extended mitochondrial targeting domain peptide. J Extracell Vesicles 2022;11:e12274
18. Burnley-Hall N, Willis G, Davis J, Rees DA, James PE. Nitrite-derived nitric oxide reduces hypoxia-inducible factor 1α-mediated extracellular vesicle production by endothelial cells. Nitric Oxide 2017;63:1-12
19. Min Lim K, Kim S, Yeom J, et al. Advanced 3D dynamic culture system with transforming growth factor-β3 enhances production of potent extracellular vesicles with modified protein cargoes via upregulation of TGF-β signaling. J Adv Res 2023;47:57-74
20. Song K, Dayem AA, Lee S, et al. Superior therapeutic activity of TGF-β-induced extracellular vesicles against interstitial cystitis. J Control Release 2022;348:924-937
21. Lim KM, Dayem AA, Choi Y, et al. High therapeutic and esthetic properties of extracellular vesicles produced from the stem cells and their spheroids cultured from ocular surgery-derived waste orbicularis oculi muscle tissues. Antioxidants (Basel) 2021;10:1292
22. van der Fits L, Mourits S, Voerman JS, et al. Imiquimod-

induced psoriasis-like skin inflammation in mice is mediated via the IL-23/IL-17 axis. J Immunol 2009;182:5836-5845
23. Wang Y, Zeng D, Wei L, et al. Effects of emulsifiers on lipid metabolism and performance of yellow-feathered broilers. BMC Vet Res 2024;20:246
24. Beutner KR, Tyring S. Human papillomavirus and human disease. Am J Med 1997;102(5A):9-15
25. Zhou X, Chen Y, Cui L, Shi Y, Guo C. Advances in the pathogenesis of psoriasis: from keratinocyte perspective. Cell Death Dis 2022;13:81
26. Dazzi F, Krampera M. Mesenchymal stem cells and autoimmune diseases. Best Pract Res Clin Haematol 2011;24:49-57
27. Kim CH, Lim CY, Lee JH, Kim KC, Ahn JY, Lee EJ. Human embryonic stem cells-derived mesenchymal stem cells reduce the symptom of psoriasis in imiquimod-induced skin model. Tissue Eng Regen Med 2018;16:93-102
28. Imai Y, Yamahara K, Hamada A, Fujimori Y, Yamanishi K. Human amnion-derived mesenchymal stem cells ameliorate imiquimod-induced psoriasiform dermatitis in mice. J Dermatol 2019;46:276-278
29. Shin L, Peterson DA. Human mesenchymal stem cell grafts enhance normal and impaired wound healing by recruiting existing endogenous tissue stem/progenitor cells. Stem Cells Transl Med 2013;2:33-42
30. Caponnetto F, Manini I, Skrap M, et al. Size-dependent cellular uptake of exosomes. Nanomedicine 2017;13:1011-1020
31. Litvinov IV, Bizet AA, Binamer Y, Jones DA, Sasseville D, Philip A. CD109 release from the cell surface in human keratinocytes regulates TGF-β receptor expression, TGF-β signalling and STAT3 activation: relevance to psoriasis. Exp Dermatol 2011;20:627-632
32. Jiang M, Sun Z, Dang E, et al. TGFβ/SMAD/microRNA-486-3p signaling axis mediates keratin 17 expression and keratinocyte hyperproliferation in psoriasis. J Invest Dermatol 2017;137:2177-2186
33. Henriet E, Abdallah F, Laurent Y, et al. Targeting TGF-β1/miR-21 pathway in keratinocytes reveals protective effects of silymarin on imiquimod-induced psoriasis mouse model. JID Innov 2022;3:100175
34. Herman A, Herman AP. Essential oils and their constituents as skin penetration enhancer for transdermal drug delivery: a review. J Pharm Pharmacol 2015;67:473-485
35. Lai RC, Tan SS, Teh BJ, et al. Proteolytic potential of the MSC exosome proteome: implications for an exosome-mediated delivery of therapeutic proteasome. Int J Proteomics 2012;2012:971907
36. Facchin BM, Dos Reis GO, Vieira GN, et al. Inflammatory biomarkers on an LPS-induced RAW 264.7 cell model: a systematic review and meta-analysis. Inflamm Res 2022;71:741-758
37. Cai Y, Xue F, Quan C, et al. A critical role of the IL-1β-IL-1R signaling pathway in skin inflammation and psoriasis pathogenesis. J Invest Dermatol 2019;139:146-156